Statistical Modeling of Atrioventricular Nodal Function During Atrial Fibrillation Focusing on the Refractory Period Estimation

Valentina D.A. Corino[1(✉)], Frida Sandberg[2], Federico Lombardi[3], Luca T. Mainardi[1], and Leif Sörnmo[2]

[1] Dipartimento di Elettronica, Informazione e Bioingegneria, Politecnico di Milano, Milan, Italy
{valentina.corino,luca.mainardi}@polimi.it
[2] Department of Biomedical Engineering and Center for Integrative Electrocardiology (CIEL), Lund University, Lund, Sweden
{frida.sandberg,leif.sornmo}@bme.lth.se
[3] UOC Malattie Cardiovascolari, Fondazione IRCCS Ospedale Maggiore Policlinico, Dipartimento di Scienze Cliniche e di Comunità, University of Milan, Milan, Italy
federico.lombardi@unimi.it

Abstract. We have recently proposed a statistical AV node model defined by a set of parameters characterizing the arrival rate of atrial impulses, the probability of an impulse passing through the fast or the slow pathway, the refractory periods of the pathways, and the prolongation of refractory periods. All parameters are estimated from the RR interval series using maximum likelihood (ML) estimation, except for the mean arrival rate of atrial impulses which is estimated by the AF frequency derived from the f-waves. In this chapter, we compare four different methods, based either on the Poincaré plot or ML estimation, for determining the refractory period of the slow pathway. Simulation results show better performance of the ML estimator, especially in the presence of artifacts due to premature ventricular beats or misdetected beats. The performance was also evaluated on ECG data acquired from 26 AF patients during rest and head-up tilt test. During tilt, the AF frequency increased (6.08 ± 1.03 Hz vs. 6.20 ± 0.99 Hz, $p < 0.05$, rest vs. tilt) and the refractory periods of both pathways decreased (slow pathway: 0.43 ± 0.12 s vs. 0.38 ± 0.12 s, $p = 0.001$, rest vs. tilt; fast pathway: 0.55 ± 0.14 s vs. 0.47 ± 0.11 s, $p < 0.05$, rest vs. tilt). These results show that AV node characteristics can be assessed non-invasively to quantify changes induced by autonomic stimulation.

Keywords: Atrial fibrillation · Atrioventricular node · Statistical modeling · Maximum likelihood estimation

1 Introduction

During atrial fibrillation (AF), atrial impulses cause summation and/or cancellation of wavefronts in the AV node, which in turn causes disorganization of the

M. Fernández-Chimeno et al. (Eds.): BIOSTEC 2013, CCIS 452, pp. 258–268, 2014.
DOI: 10.1007/978-3-662-44485-6_18

penetrating impulses so that the ventricular rhythm is more irregular than during sinus rhythm. Although AV nodal properties such as refractoriness and concealed conduction determine the characteristics of the ventricular response [1], no evaluation is performed on a routine basis in clinical practice due to the lack of suitable noninvasive methodology.

Various nonparametric approaches to the analysis of AV coupling during AF have recently been proposed, e.g., [2–4]. The Poincaré surface profile is a histographic variant of the well-known Poincaré plot introduced to filter part of the AV node memory effects, with the overall aim to detect preferential AV nodal conductions [2]. The AV synchrogram was introduced for beat-to-beat assessment of AV coupling during AF, as well as for other atrial tachyarrhythmias. This technique involves a stroboscopic observation of the ventricular phase at times triggered by atrial activations [4]. The synchrogram was found useful for tracking the time course of AV coupling and for partially reconstructing the dynamics of AV response during AF.

A number of AV node models have been proposed during the last decade where it is assumed that the atrial electrogram is available, e.g., recorded during electrophysiological studies [5,6]. Thus, these models are less suitable for use in clinical routine where it is preferable to estimate all model parameters from the surface ECG. Simulation models represent another type of model which are useful for investigating certain AV nodal characteristics [7] or the effect of pacing [8,9]. These models offer detailed characterization of the underlying electrophysiological dynamics, but do not lend themselves to analysis of real data since the number of parameters is much too large to produce estimates with sufficient accuracy.

In a recent paper [10], we have shown that statistical model-based analysis, relying entirely on information derived from the surface ECG, can be employed for evaluating essential AV nodal characteristics during AF. The model is defined by a parsimonious set of parameters which characterizes the arrival rate of atrial impulses, the probability of an impulse passing through the fast or the slow pathway, the refractory periods of the pathways, and the prolongation of refractory periods. Maximum likelihood (ML) estimation was considered for estimating the parameters from the observed RR interval series, except for the shorter refractory period, estimated from the Poincaré plot of successive RR intervals, and the mean arrival rate of atrial impulses, estimated by the AF frequency derived from the f-waves of the ECG [11]. The results, determined from a total of 2004 30-min ECG segments, selected from 36 AF patients, showed that 88 % of the segments could be accurately modeled when the estimated probability density function (PDF) and an empirical PDF were at least 80 % in agreement. The study suggested that atrial activity is an important determinant of ventricular rhythm during AF.

In a subsequent paper, we have improved the AV node model to offer a more detailed characterization of the dual pathways [12]. The estimation procedure was also improved to become more robust with respect to artifacts in the RR interval series. The results for the improved model showed a significantly better

fit between the estimated and the empirical PDF than previously reported for the original model in [10].

The goal of the present study is to compare different techniques for estimating the refractory period of the slow pathway. In particular, we compare three methods based on the Poincaré plot and one where the refractory period is estimated jointly with the ML estimation. The best-performing method (according to simulation results) is then studied on an ECG dataset recorded during rest and tilt testing.

2 Methods

2.1 AV Node Model

The AV node is treated as a lumped structure which accounts for concealed conduction, relative refractoriness, and dual AV nodal pathways [12]. Atrial impulses are assumed to arrive to the AV node according to a Poisson process with mean arrival rate λ. We assume that each arriving impulse is suprathreshold, i.e., the impulse results in ventricular activation unless blocked by a refractory AV node. The probability of an atrial impulse passing through the AV node depends on the time elapsed since the previous ventricular activation. The length of the refractory period is defined by a deterministic part τ and a stochastic part τ_p. The latter part models prolongation due to concealed conduction and/or relative refractoriness, and is assumed to be uniformly distributed in the interval $[0, \tau_p]$. Hence, all atrial impulses arriving to the AV node before the end of the refractory period τ are blocked. Then follows an interval $[\tau, \tau + \tau_p]$ with linearly increasing likelihood of penetration into the AV node. Finally, no impulses can be blocked if they arrive after the end of the maximally prolonged refractory period $\tau + \tau_p$. The mathematical characterization of refractoriness of the i:th pathway ($i = 1, 2$) is thus defined by the positive-valued function $\beta_i(t)$,

$$\beta_i(t) = \begin{cases} 0, & 0 < t < \tau_i \\ \frac{t - \tau_i}{\tau_{p,i}}, & \tau_i \leq t < \tau_i + \tau_{p,i} \\ 1, & t \geq \tau_i + \tau_{p,i}, \end{cases} \tag{1}$$

where t denotes the time elapsed since the preceding ventricular activation.

The probability of an atrial impulse to pass through the pathway with the shorter refractory period τ_1 is equal to α, and accordingly the other pathway is taken with probability $(1 - \alpha)$. For this model, the time intervals x_i between consecutive ventricular activations, i.e., corresponding to the RR intervals, are independent. It can be shown that the joint PDF is given by [10]

$$p_x(x_1, x_2, \ldots, x_M) = \prod_{m=1}^{M} (\alpha p_{x,1}(x_m) + (1 - \alpha) p_{x,2}(x_m)), \tag{2}$$

where M is the total number of intervals, and $p_{x,i}(x_m), i = 1, 2$, is given by

$$p_{x,i}(x) = \begin{cases} 0, & x < \tau_i \\ \frac{\lambda y_i}{\tau_{p,i}} \exp\left\{\frac{-\lambda y_i^2}{2\tau_{p,i}}\right\}, & \tau_i \le x < \tau_i + \tau_{p,i} \\ \lambda \exp\left\{\frac{-\lambda \tau_{p,i}}{2} - \lambda(y_i - \tau_{p,i})\right\}, & x \ge \tau_i + \tau_{p,i}. \end{cases} \tag{3}$$

where $y_i = x - \tau_i$.

2.2 Model Parameter Estimation

Interdependence of Consecutive RR Intervals. Since the property of statistical independence is not fully valid for RR intervals, a simple functional dependence of the refractory periods related to the previous RR interval is explored. The interdependence of consecutive RR intervals can be reduced by preprocessing the original RR interval series, denoted x'_m, with the linear transformation,

$$x_m = x'_m - \hat{s}_\tau x'_{m-1}, \tag{4}$$

where $\hat{s}_\tau$ is determined from the line that defines the lower envelope of the Poincaré plot.

Alternatively, the autocorrelation function of the RR intervals can be used for determining $\hat{s}_\tau$ [13]. During AF, the first lag of the autocorrelation is significant, whereas it is negligible for larger lags. Hence, decorrelation of the RR interval series is accomplished by (4), where $\hat{s}_\tau$ is taken as the smallest value in the interval $[0, 0.5]$ that makes the first lag negative.

Estimation of $\boldsymbol{\lambda}$. The atrial impulses were assumed to arrive to the AV node according to a Poisson process at a rate λ. An estimate of λ is obtained by

$$\lambda = \frac{\lambda_{\mathrm{AF}}}{1 - \delta\lambda_{\mathrm{AF}}}, \tag{5}$$

where λ_{AF} is the dominant AF frequency estimated from the ECG (independently of the AV node parameters), and δ is minimum time interval between successive impulses arriving to the AV node. Equation (5) derives from the assumption that atrial impulses do not arrive to the AV node closer to each other than at a minimum interval δ.

Estimation of Dual Pathway Parameters. The model parameters related to the dual AV nodal pathways and the refractory period prolongation, except $\tau_1^{\min}$, are estimated by maximizing the log-likelihood function $\Lambda(\boldsymbol{\theta})$ with respect to the vector $\boldsymbol{\theta}$ that contains the unknown parameters [12],

$$\hat{\boldsymbol{\theta}} = \arg\max_{\boldsymbol{\theta}} \Lambda(\boldsymbol{\theta}), \tag{6}$$

where

$$\boldsymbol{\theta} = \left[\alpha\ \tau_2^{\min}\ \tau_{p,1}\ \tau_{p,2}\right]^T. \tag{7}$$

The parameter(s) defining both a single pathway model, i.e., $\theta = \tau_{p,1}$, and a dual pathway model, i.e., the vector $\boldsymbol{\theta}$ in (7), are estimated. The Bayes information criterion is used to determine which of these two models is the most appropriate one.

Since no closed-form solution can be found for the ML estimator, combined with the fact that the gradient is discontinuous, multi-swarm particle swarm optimization (MPSO) is employed for the maximization in (6). Briefly, a multi-initialization with N concurrent swarms is employed in MPSO [14,15]. Each swarm is moved within a search area to find the optimal solution. After a certain number of optimization epochs, particles are exchanged between swarms to avoid local maxima.

Estimation of $\boldsymbol{\tau_1^{\min}}$. Four techniques for estimating the refractory period $\tau_1^{\min}$ of the slow AV pathway are compared, of which the first three methods explore the Poincaré plot in which each RR interval is plotted versus the preceding interval [16]. The resulting pattern may be used to distinguish AF from other supraventricular tachycardias such as atrial flutter with its much more regular ventricular response [17]. During AF, the irregularity of RR intervals results in a widely scattered distribution which is representative of disorganized atrial activity combined with atrioventricular conduction properties. The four techniques are now briefly described.

Linear fitting (LF) has been explored by plotting 512 points and dividing the horizontal axis into adjacent bins of 64 points [18]. The lower envelope results from a linear fit to the shortest RR intervals of all bins.

Modified linear fitting extends linear fitting by shifting the intercept of the fitted line until no points are below. This technique is motivated by the observation that the lower envelope represents the minimal refractory period.

The Hough transform is a technique for detecting straight lines in an image. Its application to the Poincaré plot in AF analysis was first pointed out in [19], see also [20]. Briefly, this plot is discretized (bin size of 20 ms) and edges are extracted using the Sobel approximation of the derivative. In the Hough space, a straight line is represented as a point, and the maximum value in this space corresponds to the most represented line in the input image. To find the lower envelope, the slope is constrained to 0–0.5 and the intercept to be positive. Among the lines satisfying these criteria, the one that is closest, in the mean square error sense, to the minimum points of the edge image is chosen.

Joint ML estimation of $\tau_1^{\min}$ and $\boldsymbol{\theta}$ was recently proposed [13]. Since the estimate of $\tau_1^{\min}$ is closely related to the shortest interval of the RR series, cf. the definition of $p_{x,i}(x)$ in (3), the handling of artifacts is important. The following iterative procedure is adopted to reduce the influence of artifactual intervals. Initially, 1 % of the shortest RR intervals are removed from the decorrelated RR interval series $\mathbf{x}$, after which ML estimation is performed on the truncated series,

denoted $\tilde{\mathbf{x}}_0$. Since $\tilde{\mathbf{x}}_0$ is assumed to be free of incorrect RR intervals, the initial estimate

$$\tilde{\boldsymbol{\theta}}_0 = \left[\alpha(0)\ \tau_1^{\min}(0)\ \tau_2^{\min}(0)\ \tau_{p,1}(0)\ \tau_{p,2}(0)\right]^T \tag{8}$$

can serve as a reference. The removed RR intervals are then brought back to the truncated series one by one in order of size so that $\tilde{\mathbf{x}}_i = \left[\tilde{\mathbf{x}}_{i-1}\, x(i)\right]$, where $x(i)$ is the longest interval removed from $\tilde{\mathbf{x}}_{i-1}$; ML estimation is performed for each $\tilde{\mathbf{x}}_i$. The estimates corresponding to the maximum value of the log-likelihood function are chosen as the final ones.

3 Data

3.1 Simulated Data

Simulated 10-min RR interval series were generated, using the AV node model introduced in [12], to test the different methods for estimating $\tau_1^{\min}$. We used 5 different parameter settings (100 runs per setting), see Table 1. To test whether the estimation of $\tau_1^{\min}$ is robust to the presence of artifacts, we introduced a fixed percentage of artifacts (0, 0.3, 0.6, and 0.9 % of the RR series length). The occurrence time was evenly distributed in the range 0.2 s–$\tau_1^{\min}$. The AF frequency λ was assumed to be known.

Table 1. Simulations parameter setting.

	Sim1	Sim2	Sim3	Sim4	Sim5
λ	6 Hz	6.5 Hz	5 Hz	6 Hz	8 Hz
α	0.8	0.5	0.4	0.3	0.7
$\tau_1^{\min}$	0.28 s	0.30 s	0.28 s	0.32 s	0.34 s
$\tau_2^{\min}$	0.35 s	0.37 s	0.40 s	0.40 s	0.43 s
$\tau_{p,1}$	0.10 s	0.20 s	0.05 s	0.10 s	0.10 s
$\tau_{p,2}$	0.15 s	0.10 s	0.05 s	0.15 s	0.10 s

3.2 Real Data

We analyzed 25 consecutive patients with persistent AF (67 ± 7 years, 16 females) who underwent electrical cardioversion, according to the international guidelines, at the Cardiology department of San Paolo Hospital, Milan, Italy. Recordings were acquired at rest and during a passive orthostatic stimulus (75° tilting). One patient was excluded from analysis due to poor ECG quality which prevented the estimation of AF frequency. Hence, the results presented below are based on 24 patients.

The ECG was recorded at rest for 10 min and, when applicable, followed by tilting, using three orthogonal leads and a sampling rate of 1 kHz. All recordings were performed in the morning in a quiet environment following 15 min of adaptation. The study was approved by the Ethics Committee, and all patients gave their written informed consent to participate.

4 Results

4.1 Simulated Data

Figure 1 shows the mean and standard deviation of $\hat{\tau}_1^{\min}$ obtained with the four methods. It can be noted that the larger the percentage of inserted artifacts, the worse perform the methods based on the Poincaré plot. On the other hand, the estimates obtained by ML estimation remain quite stable and close to the true value.

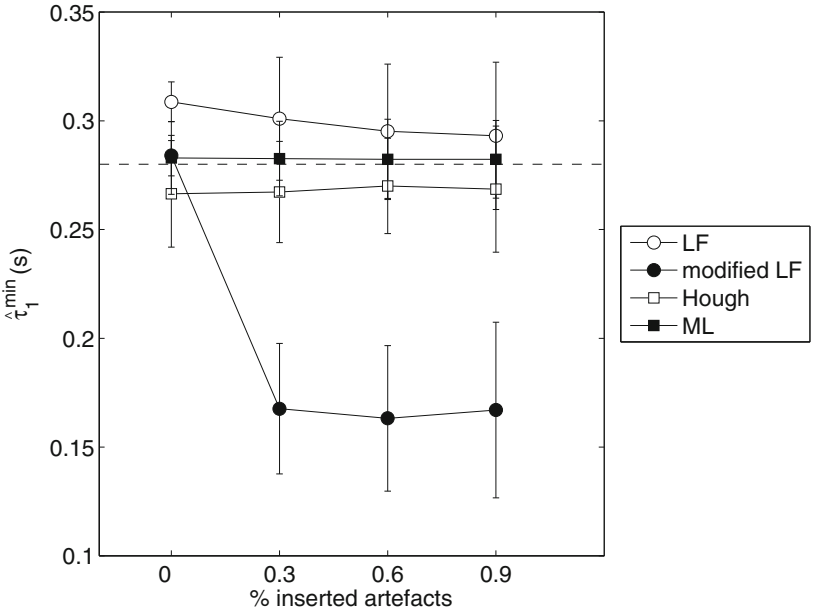

Fig. 1. Mean and standard deviation of $\hat{\tau}_1^{\min}$, computed for 100 RR series, for different percentages of inserted artifacts; the true value is indicated by the dashed line. The following model parameter values were used: $\lambda = 6$ Hz, $\tau_1^{\min} = 0.28$ s, $\tau_2^{\min} = 0.35$ s, $\alpha = 0.8$, $\tau_{p,1} = 0.1$ s, and $\tau_{p,2} = 0.15$ s.

Figure 2 shows the mean normalized absolute error between $\hat{\tau}_1^{\min}$ and the true value $\tau_1^{\min}$ averaged on the five simulation settings using the four analyzed methods. When estimating $\tau_1^{\min}$ using the ML estimation, it is observed that the error is well below 5 % even in the presence of a high percentage of artifacts.

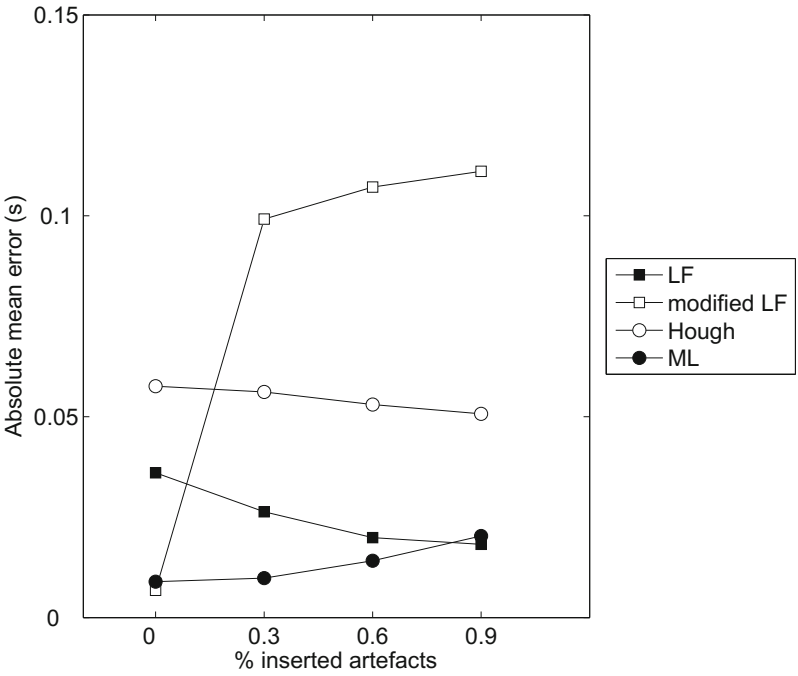

Fig. 2. The mean normalized absolute error between $\hat{\tau}_1^{\min}$ and the true value using the four methods.

4.2 Real Data

To assess whether the model parameters can capture changes due to increased sympathetic tone, e.g., observed during a tilt test, the parameter estimates obtained during rest were compared to those during tilt. Table 2 compares the model parameter estimates obtained at rest and during tilt, with significant changes due to sympathetic activation in both $\hat{\tau}_1^{\min}$ and $\hat{\tau}_2^{\min}$. The AF frequency was found to increase significantly during tilt. The probability of an atrial impulse to chose either pathway is almost equal during rest and tilt ($\alpha = 0.5$), although α spans the range from 0.05 to 1 in individual patients, thus making the involvement of the pathway with slower refractory period ($\alpha < 0.5$) in about half of all recordings. The refractory periods of both pathways are significantly shortened during tilt, whereas their prolongation remains almost unchanged.

Both the mean and standard deviation of RR intervals are significantly shortened during tilt due to sympathetic activation. The mean RR interval length was 763 ± 149 ms vs. 697 ± 135 ms (rest vs. tilt, $p < 0.0001$), and the related standard deviation was 161 ± 48 ms vs. 141 ± 32 ms (rest vs. tilt, $p < 0.0001$).

Table 2. Comparison of rest and tilt parameters (*p < 0.05, **p = 0.001).

	Rest	Tilt
$\hat{\alpha}$	0.53 ± 0.31	0.47 ± 0.33
$\hat{\tau}_1^{\min}$ (s)	0.43 ± 0.12	0.38 ± 0.12 **
$\hat{\tau}_2^{\min}$ (s)	0.55 ± 0.14	0.47 ± 0.11 *
$\hat{\tau}_{p,1}$ (s)	0.38 ± 0.32	0.31 ± 0.25
$\hat{\tau}_{p,2}$ (s)	0.22 ± 0.31	0.30 ± 0.20
$\hat{\lambda}$ (Hz)	6.08 ± 1.03	6.20 ± 0.99 *

5 Discussion and Conclusions

In this study we have compared four different methods for estimating the refractory period of the slow pathway in the presence of artifacts. As the most problematic artifacts are the ones shorter than the refractory period itself, we inserted only this type in the simulated RR series. The results showed that the estimation of refractory period of the slow pathway obtained jointly with the ML estimation offers better accuracy than the ones obtained from the Poincaré plot, independently of the ML estimation.

It is clearly desirable to include the AF frequency λ as well in the ML estimation procedure. However, the point process model is not easily extended from being entirely RR interval related to also account for information on f-waves because the f-waves need to be extracted from the ECG.

We described an AV node model defined by parameters characterizing the arrival rate of atrial impulses, the probability of an impulse choosing either one of the dual AV nodal pathways, the refractory periods of the pathways, and the prolongation of refractory periods. After the comparison made in this study, all model parameters are estimated from the RR interval series using ML estimation, except for the mean arrival rate of atrial impulses which is estimated by the AF frequency derived from the f-waves.

Considering the physiological aspects, our results indicate that tilting is associated with significant changes in AV conduction that are well-described by the model and reflected by shortening of both $\tau_1^{\min}$ and $\tau_2^{\min}$ during adrenergic activation. Thus, the present AV node model is adequate for studying and describing the functional characteristics of AV conduction in AF patients, e.g., to assess drug effect.

References

1. Fuster, V., Rydén, L.E., Cannom, D.S., Crijns, H.J., Curtis, A.B., et al.: ACC/AHA/ESC 2006 guidelines for the management of patients with atrial fibrillation: a report of the American College of Cardiology/American Heart Association task force on practice guidelines and the European Society of Cardiology committee for practice guidelines. Circ. **114**(2006), e257–e354 (2006)

2. Climent, A., de la Salud Guillem, M., Husser, D., Castells, F., Millet, J., Bollmann, A.: Poincaré surface profiles of RR intervals: a novel noninvasive method for the evaluation of preferential AV nodal conduction during atrial fibrillation. IEEE Trans. Biomed. Eng. **56**, 433–442 (2009)
3. Climent, A., Guillem, M., Husser, D., Castells, F., Millet, J., Bollmann, A.: Role of atrial rate as a factor modulating ventricular response during atrial fibrillation. PACE **15**, 1–8 (2010)
4. Masè, M., Glass, L., Disertoric, M., Ravelli, F.: The AV synchrogram: a novel approach to quantify atrioventricular coupling during atrial arrhythmias. Biomed. Signal Proc. Control **8**, 1008–1016 (2013)
5. Jørgensen, P., Schäfer, C., Guerra, P.G., Talajic, M., Nattel, S., Glass, L.: A mathematical model of human atrioventricular nodal function incorporating concealed conduction. Bull. Math. Biol. **64**, 1083–1099 (2002)
6. Mangin, L., Vinet, A., Page, P., Glass, L.: Effects of antiarrhythmic drug therapy on atrioventricular nodal function during atrial fibrillation in humans. Europace **7**, S71–S82 (2005)
7. Rashidi, A., Khodarahmi, I.: Nonlinear modeling of the atrioventricular node physiology in atrial fibrillation. J. Theor. Biol. **232**, 545–549 (2005)
8. Lian, J., Müssig, D., Lang, V.: Computer modeling of ventricular rhythm during atrial fibrillation and ventricular pacing. IEEE Trans. Biomed. Eng. **53**, 1512–1520 (2006)
9. Lian, J., Müssig, D.: Heart rhythm and cardiac pacing: an integrated dual-chamber heart and pacer model. Ann. Biomed. Eng. **37**, 64–81 (2009)
10. Corino, V.D.A., Sandberg, F., Mainardi, L.T., Sörnmo, L.: An atrioventricular node model for analysis of the ventricular response during atrial fibrillation. IEEE Trans. Biomed. Eng. **58**, 3386–3395 (2011)
11. Sandberg, F., Stridh, M., Sörnmo, L.: Frequency tracking of atrial fibrillation using hidden Markov models. IEEE Trans. Biomed. Eng. **55**, 502–511 (2008)
12. Corino, V.D.A., Sandberg, F., Mainardi, L.T., Sörnmo, L.: Atrioventricular nodal function during atrial fibrillation: model building and robust estimation. Biomed. Signal Proc. Control **8**, 1017–1025 (2013)
13. Corino, V.D.A., Sandberg, F., Mainardi, L.T., Sörnmo, L.: Statistical modeling of the atrioventricular node during atrial fibrillation: data length and estimator performance. In: Proceedings of 2013 35th Annual International Conference of the IEEE Engineering in Medicine and Biology Society (EMBC). vol. 35, pp. 2567–2570 (2013)
14. Van den Bergh, F., Engelbrecht, A.P.: A cooperative approach to particle swarm optimization. IEEE Trans. Evol. Comput. **8**, 225–239 (2004)
15. Niu, B., Zhu, Y., He, X., Wu, H.: MCPSO: a multi-swarm cooperative particle swarm optimizer. Appl. Math. Comput. **2**, 1050–1062 (2007)
16. Brennan, M., Palaniswami, M., Kamen, P.: Do existing measures of Poincaré plot geometry reflect nonlinear features of heart rate variability? IEEE Trans. Biomed. Eng. **48**, 1342–1347 (2001)
17. Anan, T., Araki, K.S.H., Nakamura, M.: Arrhythmia analysis by successive RR plotting. J. Electrocardiol. **23**, 243–248 (1990)
18. Hayano, J., Sakata, S., Okada, A., Mukai, S., Fujinami, T.: Circadian rhythms of atrioventricular conduction properties in chronic atrial fibrillation with and without heart failure-relation between mean heart rate and measures of heart rate variability. J. Am. Coll. Cardiol. **31**, 158–166 (1998)

19. Corino, V.D.A., Climent, A., Mainardi, L.T., Bollmann, A.: Analysis of ventricular response during atrial fibrillation. In: Mainardi, L.T., Sörnmo, L., Cerutti, S. (eds.) Understanding Atrial Fibrillation: The Signal Processing Contribution. Morgan and Claypool (2008)
20. Corino, V.D.A., Sandberg, F., Mainardi, L.T., Sörnmo, L.: Non-invasive, robust estimation of refractory period of atrioventricular node during atrial fibrillation. Int. J. Bioelectromagnetism **15**, 41–46 (2013)